PROCEEDINGS OF SCIENCE

Measuring the CKM matrix element V_{td} and V_{ts} at the electron proton colliders

Hao Sun*
Institute of Theoretical Physics, School of Physics,
Dalian University of Technology,
No.2 Linggong Road, Dalian, Liaoning, 116024, P.R.China
E-mail: haosun@dlut.edu.cn, haosun@mail.ustc.edu.cn

In this talk we present a study on the measurement of V_{td} and V_{ts} CKM matrix elements, at the future electron proton colliders, through W boson and bottom quark associated production channels as well as W boson and jet associated production channels. The W and bottom (jet) final states can be produced by s-channel single top decay or t-channel top exchange. We find that these channels provide very good prospects for a measurement of V_{td} and V_{ts} CKM matrix elements for the LHC based electron proton collider.

XXVI International Workshop on Deep-Inelastic Scattering and Related Subjects (DIS2018)
16-20 April 2018
Kobe, Japan

*Speaker.

PoS(DIS2018)167

1. Introduction

According to the standard model (SM), quarks come in three generations, with up and down type flavors. The weak charged current for quarks can be written as $J^{\mu+}_{qW} = \frac{1}{\sqrt{2}}\bar{U}_L\gamma^\mu V D_L$. Here $Q_L = \frac{1}{2}(1-\gamma^5)Q$, indicates the left-handed projection. V is the Cabibbo-Kobayashi-Maskawa (CKM) matrix [1, 2], governing flavor transitions among quarks and describing how the mass states are mixed. The conventional labeling for the flavor mixing matrix is

$$V = \begin{pmatrix} V_{ud} & V_{us} & V_{ub} \\ V_{cd} & V_{cs} & V_{cb} \\ V_{td} & V_{ts} & V_{tb} \end{pmatrix}. \tag{1.1}$$

The SM itself does not predict the elements of V, thus they should be evaluated experimentally.

Currently the first two rows of V are already being probed directly with improving precision, mainly through decays of nuclei, pions, kaons, hyperons, charmed mesons and B-hadrons. On the other hand, few direct experimental measurements exist regarding the third row of V, describing couplings of the top quark. The best method to independently measure V_{tb} is in single top production at the LHC. The remaining third row elements V_{td} and V_{ts} are very small, and it is experimentally difficult to precisely measure the $t \to d$ and $t \to s$ transitions in the single top production at the LHC, therefore few information can be obtained in this direct measurement channel. Instead, they are currently derived from CKM unitarity considerations, and are best measured indirectly in virtual processes with loop diagrams involving top quarks, giving rise to, for example, $B^0-\bar{B}^0$ or $B^0_s-\bar{B}^0_s$ mixing. A global CKM fit in Ref.[3] yields $|V^{fit}_{tb}| = 1-8.81^{+0.12}_{-0.24}\times10^{-3}$, $|V^{fit}_{ts}| = 41.08^{+3.0}_{-5.7}\times10^{-3}$, $|V^{fit}_{td}| = 8.575^{+0.076}_{-0.098}\times10^{-3}$. Notice the CKM unitarity assumption, as well as the SM contributions in the third row elements determinations in the loop induced rare flavor processes, are not valid if beyond SM physics are considered. Therefore, performing direct measurements to confirm the values of these CKM elements is very interesting and important.

Here we study the prospects to extract V_{td} and V_{ts} elements through single top related productions at the electron proton (ep) colliders, for example, the Large Hadron Electron Collider (LHeC), based on the current running machine LHC. The point is that, charged current single top production is the dominant production channel at the ep colliders involving V_{tx} vertices, while the top pair background is suppressed. This is not like the situation at the LHC, where top pair production has a very large cross section and constitutes a dangerous background for single top production. We organize our talk as follows. In Section 2 we study the signal production and backgrounds. In Section 3 we provide the limits on the matrix elements. Finally we ends with a short summary.

2. THE MEASUREMENT STRATEGY

Following Ref.[4], we will parameterize eventual deviations from the fitted number in the CKM matrix element V_{td} and V_{ts} through the ratio $R_d = |V_{td}|/|V^{fit}_{td}|$ and $R_s = |V_{ts}|/|V^{fit}_{ts}|$, in order to classify processes according to their leading power in the parameters R_d and R_s. In our study we concentrate on the charged current single top mechanism which is actually the dominant top

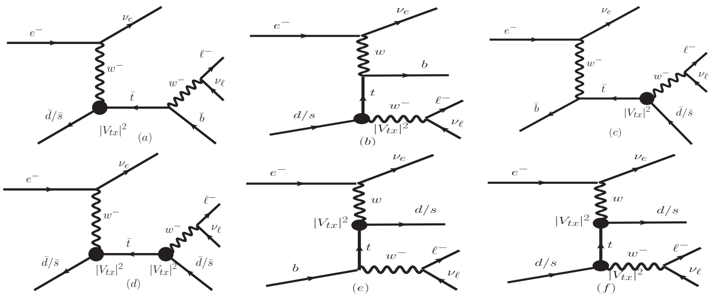

Figure 1: Feynman diagrams for different signal channels that involving V_{tx} vertex.

related channel at the ep colliders, where the signals are

$$\begin{aligned}
\text{Signal.1}: &\quad pe^- \to \nu_e \bar{t} \to \nu_e W^- \bar{b} \to \nu_e \ell^- \nu_\ell \bar{b}, \\
\text{Signal.2}: &\quad pe^- \to \nu_e W^- b \to \nu_e \ell^- \nu_\ell b, \\
\text{Signal.3}: &\quad pe^- \to \nu_e \bar{t} \to \nu_e W^- j \to \nu_e \ell^- \nu_\ell j, \\
\text{Signal.4}: &\quad pe^- \to \nu_e W^- j \to \nu_e \ell^- \nu_\ell j.
\end{aligned} \tag{2.1}$$

The Feynman diagrams that involving at least one V_{tx} vertex are shown in Fig.1. In order to

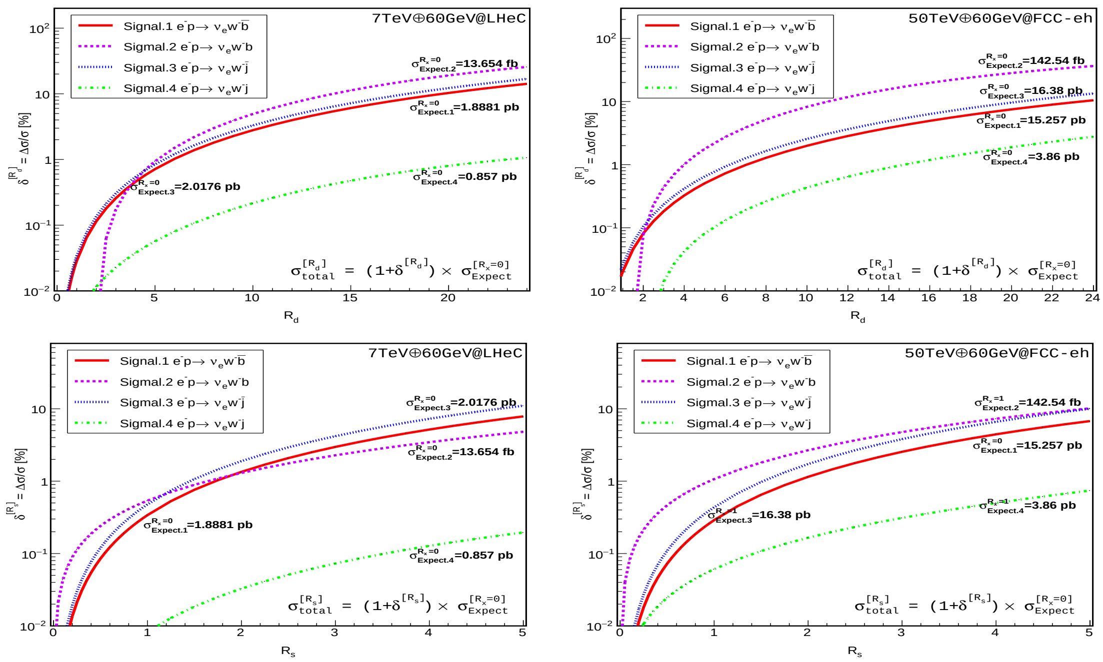

Figure 2: Signal production rate for different channels.

compare the production rate for different signal channels, we present some numerical results in Fig.2. Some basic cuts are applied here, like the transverse momentum of jets $p_T^{b(j)}$ should be larger than 20(10) GeV. The W boson is, here, not asked to be decayed. To show the pure signal contributions from the V_{tx} vertex, we do like this: we produce the production rate with $R_{d(s)}$ equal exactly zero and obtain the cross section that we expect ($\sigma_{\text{Expect}}^{R_x=0}$). By varying the R parameter, we obtain the total cross section ($\sigma^{\mathrm{R_x}}_{\mathrm{total}}$). The pure signal contribution can therefore be written as

$$\sigma^{[\mathrm{R_x}]}_{\mathrm{Signal}} = \delta^{[\mathrm{R_x}]} \times \sigma^{[\mathrm{R_x}=0]}_{\mathrm{Expect}} \quad \text{where} \quad \delta^{[\mathrm{R_x}]} = \frac{\sigma^{[\mathrm{R_x}]}_{\mathrm{total}} - \sigma^{[\mathrm{R_x}=0]}_{\mathrm{Expect}}}{\sigma^{[\mathrm{R_x}=0]}_{\mathrm{Expect}}}. \tag{2.2}$$

The δ dependence as functions of R parameters are shown in Fig.2. The solid red, dashed purple, dotted blue and dash-dotted green curve correspond to Signal.1, 2, 3, 4 respectively. The numerical results of $\sigma^{[\mathrm{R_x}=0]}_{\mathrm{Expect}}$ can be found in Tab.1, and also shown in Fig.2. From Fig.2, we see that the en-

$\sigma^{[\mathrm{R_x}=0]}_{\mathrm{Expect}}$	7TeV⊕60GeV@LHeC	50TeV⊕60GeV@FCC-eh
Signal.1	1.8881 pb	15.257 pb
Signal.2	13.654 fb	142.54 fb
Signal.3	2.0176 pb	16.38 pb
Signal.4	0.857pb	3.86 pb

Table 1: $\sigma^{[\mathrm{R_x}=0]}_{\mathrm{Expect}}$ values for different signal channels.

hancement for Signal.4 corresponding to its expected value is much smaller than the other signals, which means it's challenge to use signal.4 to have a better signal over background ratio or signal significance. For Signal.1, 2, 3, the enhanced behaviours are similar, and large, to some typical R parameters, they can reach around 10 percent. Notice in this case, Signal.1 and 3 have much larger expected cross section than Signal.2, which means they can have larger signal statistics. However, large expected cross section also means large SM backgrounds. So until now, it's still difficult to say which channel is the best one among Signal.1, 2 and 3, and a more detailed analysis on the backgrounds is also required. The corresponding backgrounds we considered are

$$\mathrm{B1:}\ \mathrm{pe^-} \to \nu_e \bar{\mathrm{t}} \to \nu_e \mathrm{W^-} \bar{\mathrm{b}} \to \nu_e \ell^- \nu_\ell \bar{\mathrm{b}}. \tag{2.3}$$

where the W and $\bar{\mathrm{b}}$ quark are associated produced through s-channel anti-top decay.

$$\mathrm{B2:}\ \mathrm{pe^-} \to \ell^- \mathrm{E_T^{miss}} \mathrm{b}/\bar{\mathrm{b}}, \tag{2.4}$$

which produced from different sources including a) $\mathrm{pe^-} \to \nu_e \mathrm{W^-b} \to \nu_e \ell^- \nu_\ell \mathrm{b}$ with t-channel top quark exchanging. In this case, the final state has a bottom quark, instead of an anti-bottom quark as in B1. Notice this one is in fact not possible to be separated from B1 since it is currently not possible to identify jets with their charges. b) $\mathrm{pe^-} \to \nu_e \mathrm{W^-b}/\bar{\mathrm{b}} \to \nu_e \ell^- \nu_\ell \mathrm{b}/\bar{\mathrm{b}}$ where the W boson and the bottom/anti-bottom are not from the s-channel anti-top decays. c) $\mathrm{pe^-} \to \mathrm{e^-Zb}/\bar{\mathrm{b}} \to \mathrm{e^-} \nu_\ell \bar{\nu}_\ell \mathrm{b}/\bar{\mathrm{b}}$, which include Z boson decays to undetected neutrinos. d) Other diagrams that belong to non-resonance contributions. There are also backgrounds, which can be formulated as

$$\mathrm{B3:}\ \mathrm{pe^-} \to \ell^- \mathrm{E_T^{miss}} \mathrm{j}, \tag{2.5}$$

due to a mistagging of the light jets to b-jets. There are some other backgrounds, like undetected particles fake missing energy, top pair background which are very small and safely ignored.

In order to provide a detector level study, we start our simulation chain with the event generator MadGraph5_aMC@NLO [6], followed by applying Pythia [7], where parton showering and hadronization is then performed. A modified version of Pythia should be used to simulate an authentic electron proton collisions. Delphes [8] is used for detector simulation. The detector is assumed based on the LHeC detector design [9, 10].

3. THE MEASUREMENT POTENTIAL

In order to present our results on the future reach of the ep colliders including systematical uncertainties, we adopt the final definition of significance as follows

$$\mathrm{SS} = \mathrm{N_s}/\sqrt{\mathrm{N_b} + (\Delta_\mathrm{B} \times \mathrm{N_b})^2} \tag{3.1}$$

where Δ_B refers to the corresponding percentage systematic uncertainties. For our signal channels, we have taken $\Delta_B = 5\%$. For the electron polarization effects, we consider it to be 80%. The 2σ limits of the $\mathrm{V_{tx}}$ value as functions of the luminosities are summarized in Fig.3. The limits from

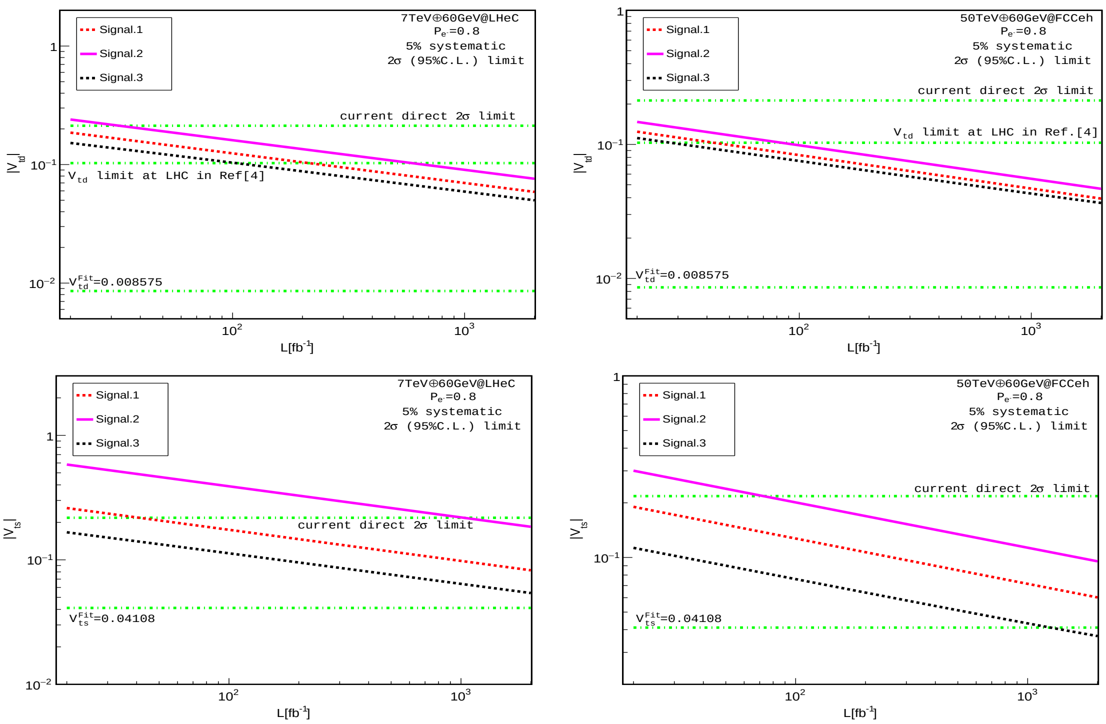

Figure 3: The 2σ limit of the $\mathrm{V_{tx}}$ value as functions of the luminosities for different signal channels.

Signal.4 is ignored due to its poor search potential. The first two figures in Fig.3 are for the $\mathrm{V_{td}}$ measurement. The dashed red(solid volet) curves are for Signal.1(2) and dashed black curve is for Signal.3 respectively. We find even at the LHeC, the limits we obtained are much lower than the current direct limits from the LHC experiment (see the upper dash-dotted curve in this figures), and comparable to, or lower than the $\mathrm{V_{td}}$ limit achieved from other phenomenological study [4] (see the middle dash-dotted curve in the first two figures in Fig.3). The measurement potential is much improved at the FCC-eh. The situation is almost the same for the measurement of $\mathrm{V_{ts}}$ which are shown in the last two figures in Fig.3. In this case, these three channels show nice feature to measure it, both at the LHeC and FCC-eh. We also notice that in all cases, Signal.3 is the most prompt channel in measuring V_{tx} elements.

Considering the proposed $2ab^{-1}$ luminosity and 80% electron polarization, the 2σ limits for R_{td} parameters for Signal.1, 2, 3 are 6.86, 8.85, 5.83 at the LHeC and 4.6, 5.44, 4.27 at the FCC-eh, correspond to the limits of V_{td} equal 0.0588, 0.0759 0.05 at the LHeC and 0.0394, 0.0466, 0.0366 at the FCC-eh. For R_{ts}, the 2σ R parameter limits are 2.01, 4.49, 1.32 at the LHeC and 1.47, 2.32, 0.90 at the FCC-eh, correspond to the limits of V_{ts} equal 0.0824, 0.1843, 0.0541 at the LHeC and 0.0602, 0.0952, 0.0369 at the FCC-eh.

4. SUMMARY

In this talk we present a study on the measurement of V_{td} and V_{ts} CKM matrix elements at the ep colliders, through W and bottom associated production channels as well as W and jet associated production channels. The W and bottom (jet) final states can be produced by s-channel single top decay or t-channel top exchange. We present the measurement potential by using different channels separately, depending on the possibility to distinguish them kinematically, but the same final state contributions are fully considered when considering different channels. In summary for the conclusion, the ep colliders provide nice features in measuring V_{td} and V_{ts} CKM matrix elements.

References

[1] N. Cabibbo, *Unitary symmetry and leptonic decays*, Phys. Rev. Lett. 10 (12) (1963) 531-533.

[2] M. Kobayashi, T. Maskawa, *CP-violation in the renormalizable theory of weak interaction*, Progress of Theoretical Physics 49 (2) (1973) 652-657.

[3] J. Charles et al., *Current status of the Standard Model CKM fit and constraints on ΔF=2 New Physics*, Phys. Rev. D 91, 073007 (2015), [arXiv:1501.05013].

[4] Ezequiel Alvarez, Leandro Da Rold, Mariel Estevez and Jernej F. Kamenik, *Measuring $|V_{td}|$ at LHC*, Phys. Rev. D 97, 033002 (2018), [arXiv:1709.07887].

[5] V. Khachatryan et al. (CMS), *Measurement of the ratio $B(t \to Wb)/B(t \to Wq)$ in pp collisions at $\sqrt{s}$=8TeV* Phys. Lett. B736, 33 (2014), arXiv:[1404.2292].

[6] J. Alwall et al., *The automated computation of tree-level and next-to-leading order differential cross sections, and their matching to parton shower simulations*, JHEP 07 (2014) 79, [arXiv:1405.0301].

[7] T. Sjostrand, S. Mrenna and P. Skands, *A brief Introduction to PYTHIA8.1*, Comput. Phys. Commun. 178 (2008) 852, [arXiv:0710.3820].

[8] J. de Favereau *et al.* [DELPHES 3 Collaboration], *DELPHES 3, A modular framework for fast simulation of a generic collider experiment*, JHEP **1402** (2014) 057, [arXiv:1307.6346].

[9] J. L. Abelleira Fernandez, et al., [LHeC Study Group Collaboration], *A Large Hadron Electron Collider at CERN: Report on the Physics and Design Concepts for Machine and Detector*, J. Phys. G 39 (2012) 075001, [arXiv:1206.2913].

[10] M. Klein, *LHeC Detector Design*, 25th International Workshop on Deep Inelastic Scattering, 2017, Birmingham, https://indico.cern.ch/event/568360/contributions/2523637/.